# research papers

# Solid-state structures of group 1 and group 2 metal 1,5-naphthalenedisulfonates: systematic investigation of lamellar three-dimensional networks constructed by metal arenedisulfonate

**Jiwen Cai,\* Cai-Hong Chen, Cheng-Zhu Liao, Xiao-Long Feng and Xiao-Ming Chen**

Instrumentation Analysis and Research Center and Department of Chemistry, Zhongshan University, Guangzhou 510275, People's Republic of China

Correspondence e-mail: puscjw@zsu.edu.cn

Seven Group 1 and Group 2 1,5-naphthalenedisulfonates (1,5-nds) have been synthesized and structurally characterized by single-crystal X-ray diffraction, IR spectroscopy and thermal gravimetric analysis. For Group 1 metal complexes, with $M = Li^+$ (1), $Na^+$ (2) and $K^+$ (3), all crystallize in the same space group ($P2_1/c$) with the same composition, $[M_2(1,5\text{-nds})(H_2O)_2]$. They adopt similar three-dimensional packing arrangements with the metal–sulfonate inorganic layers pillared by naphthalene rings. However, the coordination behavior of three metal cations toward the $SO_3^-$ group and water molecule are different, resulting in different architectures for the inorganic portion. For Group 2 complexes with $M = Mg^{2+}$ (4), $Ca^{2+}$ (5), $Sr^{2+}$ (6) and $Ba^{2+}$ (7), $Mg^{2+}$ shows no direct coordination by the $SO_3^-$ group while $Ca^{2+}$ is coordinated by four $SO_3^-$ groups and a two-dimensional network is formed. Complexes (6) and (7) are isostructural, adopting the same three-dimensional, inorganic–organic pillared framework as seen for (1)–(3). The coordination behavior of the metal cations in these structures neatly illustrates the increase in coordination strength with decreasing charge/radius ratio for Group 1 and Group 2 metal cations with large organic anions.

## 1. Introduction

Special attention has been devoted to metal organophosphates since they usually adopt a lamellar organic–inorganic network in which the metal phosphate generates the inorganic layer while the organic groups orient themselves above and below the inorganic sheet, thus constructing a porous network with promising application in catalysis, sorption, ion exchange and intercalation (Thompson, 1994). Recently, by utilizing diphosphonic acids rather than monophosphonic acids, an interesting new series of compounds with three-dimensional structures was obtained, in which the inorganic layers are connected to each other by the bifunctional alkylene (Poojary *et al.*, 1997, and references cited therein) or aromatic (Poojary *et al.*, 1996) groups, generating open spaces whose sizes are determined by the length of the organic group. Thus, a new class of pillared materials with definable cavity sizes and chemical properties may be prepared, which opens up a new research area with extensive possibilities (Poojary *et al.*, 1997, and references cited therein).

Surprisingly, the coordination chemistry of metal sulfonates remains less well explored (Sundberg & Sillanpää, 1993; Alcock *et al.*, 1993) and, consequently, less well rationalized. Lamellar inorganic–organic systems employing sulfonates are virtually unknown (Shimizu *et al.*, 1998; Shimizu, Enright, Ratcliffe, Preston *et al.* 1999; Shimizu, Enright, Ratcliffe &

Ripmeester, 1999). Attempts have been made to generate structural analogues of the layered metal phosphates (Kosnic *et al.*, 1992; Gunderman *et al.*, 1997; Shubnell *et al.*, 1994; Gunderman & Squattrito, 1994, 1995). However, due to the weak coordination strength of the sulfonate, compared with those of the phosphates, the reported metal sulfonates were all segregated inorganic–organic structures formed by extensive hydrogen-bonding interactions, instead of forming well ordered, inorganic–organic layered structures. Only very recently the first example of a functional pillared metal sulfonate network was reported (Côté & Shimizu, 2001), as well as the first nonlayered metal sulfonate structure (Yu *et al.*, 2001).

In our previous studies, by incorporating organic ligands such as ethylenediamine and *N*-methylethylenediamine at the divalent transition metal center, we succeeded in obtaining complex systems where one of the $SO_3^-$ oxygens is coordinated to $Cu^{2+}$ even in the presence of water molecules (Cai *et al.*, 2001). Therefore, the coordination behavior of the metal ions toward $SO_3^-$ can be tailored chemically and this observation prompted us to systematically investigate the structural chemistry of metal sulfonates, targeting new types of metal–organic porous compounds. Herein we report the solid-state structures of Group 1 and Group 2 metal 1,5-naphthalenedi-sulfonate (1,5-nds), namely $[M_2(1,5\text{-nds})(H_2O)_2]$ [$M$ = Li$^+$ (1), Na$^+$ (2), K$^+$ (3)] and $[M(1,5\text{-nds})(H_2O)_n]$ [$M$ = Mg$^{2+}$ (4), Ca$^{2+}$ (5), Sr$^{2+}$ (6), Ba$^{2+}$ (7)]. Interestingly, all these Group 1 [(1)–(3)] and two of the Group 2 metal naphthalenedisulfonates [(6)–(7)] form pillared three-dimensional networks, reminiscent of the reported metal biphosphate compounds (Poojary *et al.*, 1996). However, the metal ion is coordinated by the $SO_3^-$ group in different modes, demonstrating satisfactorily the increase in coordination strength associated with decreasing charge/radius ratio, a phenomenon which is well known (Cotton & Wilkinson, 1988), although less well demonstrated and documented with large organic anions.

## 2. Crystallography

Experimental details of the X-ray analyses are provided in Table 1.[1] All diffraction data were collected on a Bruker SMART1000 CCD diffractometer with graphite-mono-chromated Mo $K\alpha$ radiation ($\lambda$ = 0.71073 Å) at room temperature (Bruker 1998*a*, 1999). Absorption corrections were applied (Blessing, 1995; Bruker, 1999). The space groups were determined from systematic absences and confirmed by the results of refinement. In all cases the structures were solved by direct methods and refined using full-matrix least-squares/difference Fourier techniques (Sheldrick, 1997; Bruker, 1998*b*). All non-H atoms were refined with aniso-tropic displacement parameters and all H atoms of the ligands were placed at idealized positions and refined riding ($x$, $y$, $z$, $U_{iso}$) on their carrier atoms. Water H atoms were located from

difference Fourier maps at the final stage of refinement. The maximum peak in the final difference Fourier map of the Ba$^{2+}$ salt (7) is located 0.87 Å away from the heavy atom. Selected bond lengths and angles are listed in Table 2.

## 3. Syntheses and analyses

All materials were commercially available and were used as received. FTIR spectra were acquired as KBr pellets on a Bruker EQUINOX 55 FTIR spectrometer. Thermogravi-metric data were obtained on a Netzsch DSC-204 analyzer in flowing nitrogen. Elemental analyses were carried out with a Perkin–Elmer 240 elemental analyzer.

### 3.1. [Li$_2$(1,5-nds)(H$_2$O)$_2$] (1)

Lithium sulfate monohydrate (1.27 g, 1 mmol) and 1,5-naphthalenedisulfonic acid (0.18 g, 0.5 mmol) were dissolved in distilled water (20 ml). The resulting solution was allowed to stand in an open beaker at room temperature. After ∼10 d plate-like colorless crystals of (1) were collected (yield 57%, based on Li$_2$SO$_4$·H$_2$O: found: C 35.47, H 3.04; C$_{10}$H$_{10}$Li$_2$O$_8$S$_2$ requires C 35.73, H 3.00%). TGA: release of the coordinated water molecule at 382–401 K, 6.76% (calc. 10.71%), removal of naphthalene group at 878–887 K.

### 3.2. [Na$_2$(1,5-nds)(H$_2$O)$_2$] (2)

Sodium chloride (0.58 g, 1 mmol) and 1,5-nds acid (0.18 g, 0.5 mmol) were dissolved in distilled water (20 ml). The resulting solution was allowed to stand in an open beaker at room temperature. After ∼5 d plate-like colorless crystals of (2) were collected (yield 38%, based on NaCl; found: C 32.67, H 2.74; C$_{10}$H$_{10}$Na$_2$O$_8$S$_2$ requires C 32.61, H 2.74%). The same crystals were also obtained from water–ethanol (1:1) mixed solvent, as well as from 95% ethanol solution. TGA: release of coordinated water molecule at 358–656 K, 10.21% (calc. 9.77%), removal of naphthalene group at 885 K.

### 3.3. [K$_2$(1,5-nds)(H$_2$O)$_2$] (3)

Potassium chloride (0.75 g, 1 mmol) and 1,5-nds acid (0.18 g, 0.5 mmol) were dissolved in distilled water (20 ml). The resulting solution was allowed to stand in an open beaker at room temperature. After ∼5 d plate-like colorless crystals of (3) were collected (yield 50%, based on KCl; found: C 30.18, H 2.54; C$_{10}$H$_{10}$K$_2$O$_8$S$_2$ requires C 29.99, H 2.52%). TGA: release of water molecule at 332–350 K, 5.90% (calc. 8.99%), removal of naphthalene at 843–891 K.

### 3.4. [Mg(H$_2$O)$_6$](1,5-nds) (4)

Magnesium chloride hexahydrate (0.21 g, 1 mmol) was dissolved in distilled water (10 ml), to which disodium 1,5-nds (0.33 g, 1 mmol) was added. The resulting solution was allowed to stand at room temperature in an open beaker. After ∼3 d plate-like colorless crystals of (4) were collected (yield 33%, based on MgCl$_2$·6H$_2$O; found: C 28.58, H 4.42, S 15.67; C$_{10}$H$_{18}$O$_{12}$S$_2$Mg requires C 28.69, H 4.33, S 15.32%).

**Table 1**
Experimental details.

| | (1) | (2) | (3) | (4) |
|---|---|---|---|---|
| **Crystal data** | | | | |
| Chemical formula | $C_{10}H_{10}Li_2O_8S_2$ | $C_{10}H_{10}Na_2O_8S_2$ | $C_{10}H_{10}K_2O_8S_2$ | $C_{10}H_{18}MgO_{12}S_2$ |
| Chemical formula weight | 336.18 | 368.28 | 400.5 | 418.67 |
| Cell setting, space group | Monoclinic, $P2_1/c$ | Monoclinic, $P2_1/c$ | Monoclinic, $P2_1/c$ | Monoclinic, $P2_1/c$ |
| $a, b, c$ (Å) | 10.8901 (17), 7.8842 (13), 8.0619 (13) | 11.6398 (17), 5.5507 (8), 10.7148 (16) | 11.0278 (18), 8.5748 (14), 7.9845 (13) | 13.1955 (8), 6.6981 (4), 9.6616 (6) |
| $\beta$ (°) | 104.228 (3) | 96.187 (3) | 102.631 (3) | 92.304 (1) |
| $V$ (Å$^3$) | 670.96 (19) | 688.24 (17) | 736.8 (2) | 853.25 (9) |
| $Z$ | 2 | 2 | 2 | 2 |
| $D_x$ (Mg m$^{-3}$) | 1.664 | 1.777 | 1.805 | 1.630 |
| Radiation type | Mo $K\alpha$ | Mo $K\alpha$ | Mo $K\alpha$ | Mo $K\alpha$ |
| $\theta$ range (°) | 4.44–30.04 | 4.42–28.28 | 4.27–30.05 | 4.34–29.98 |
| $\mu$ (mm$^{-1}$) | 0.432 | 0.487 | 0.962 | 0.409 |
| Temperature (K) | 293 (2) | 293 (2) | 293 (2) | 293 (2) |
| Crystal form, color | Plate, colorless | Block, colorless | Block, colorless | Plate, colorless |
| Crystal size (mm) | $0.33 \times 0.21 \times 0.06$ | $0.33 \times 0.16 \times 0.11$ | $0.36 \times 0.20 \times 0.17$ | $0.27 \times 0.21 \times 0.19$ |
| **Data collection** | | | | |
| Diffractometer | Bruker Smart 1000 CCD area detector | Bruker Smart 1000 CCD area detector | Bruker Smart 1000 CCD area detector | Bruker Smart 1000 CCD area detector |
| Data collection method | Phi and omega scans | Phi and omega scans | Phi and omega scans | Phi and omega scans |
| No. of measured, independent and observed parameters | 4629, 1940, 1727 | 4234, 1692, 1516 | 5435, 2131, 1860 | 5674, 2449, 2250 |
| Criterion for observed reflections | $I > 2\sigma(I)$ | $I > 2\sigma(I)$ | $I > 2\sigma(I)$ | $I > 2\sigma(I)$ |
| $R_{int}$ | 0.0183 | 0.0263 | 0.0218 | 0.0188 |
| $\theta_{max}$ (°) | 30.04 | 28.28 | 30.05 | 29.98 |
| Range of $h, k, l$ | $-13 \rightarrow h \rightarrow 15$ $-9 \rightarrow k \rightarrow 11$ $-10 \rightarrow l \rightarrow 11$ | $-15 \rightarrow h \rightarrow 15$ $-5 \rightarrow k \rightarrow 7$ $-12 \rightarrow l \rightarrow 14$ | $-15 \rightarrow h \rightarrow 15$ $-12 \rightarrow k \rightarrow 5$ $-11 \rightarrow l \rightarrow 11$ | $-14 \rightarrow h \rightarrow 18$ $-9 \rightarrow k \rightarrow 9$ $-11 \rightarrow l \rightarrow 13$ |
| **Refinement** | | | | |
| Refinement on | $F^2$ | $F^2$ | $F^2$ | $F^2$ |
| $R[F^2>2\sigma(F^2)]$, $wR(F^2)$, $S$ | 0.0349, 0.1006, 1.11 | 0.0311, 0.0918, 1.056 | 0.033, 0.0939, 1.099 | 0.0282, 0.0858, 1.049 |
| No. of reflections and parameters used in refinement | 1940, 108 | 1692, 109 | 2131, 109 | 2449, 152 |
| H-atom treatment | Mixed | Mixed | Mixed | Mixed |
| Weighting scheme | $w = 1/[\sigma^2(F_o^2) + (0.0612P)^2 + 0.1528P]$, where $P = (F_o^2 + 2F_c^2)/3$ | $w = 1/[\sigma^2(F_o^2) + (0.0547P)^2 + 0.2432P]$, where $P = (F_o^2 + 2F_c^2)/3$ | $w = 1/[\sigma^2(F_o^2) + (0.0422P)^2 + 0.4224P]$, where $P = (F_o^2 + 2F_c^2)/3$ | $w = 1/[\sigma^2(F_o^2) + (0.0591P)^2 + 0.1019P]$, where $P = (F_o^2 + 2F_c^2)/3$ |
| $(\Delta/\sigma)_{max}$ | 0.001 | 0.012 | 0.000 | 0.000 |
| $\Delta\rho_{max}$, $\Delta\rho_{min}$ (e Å$^{-3}$) | 0.448, $-0.593$ | 0.356, $-0.485$ | 0.366, $-0.372$ | 0.408, $-0.363$ |
| Extinction method | None | SHELXL97 (Sheldrick, 1997) | SHELXL97 (Sheldrick, 1997) | SHELXL97 (Sheldrick, 1997) |
| Extinction coefficient | – | 0.164 (9) | 0.065 (4) | 0.083 (5) |

| | (5) | (6) | (7) |
|---|---|---|---|
| **Crystal data** | | | |
| Chemical formula | $C_{10}H_{10}CaO_8S_2$ | $C_{10}H_8O_7S_2Sr$ | $C_{10}H_8BaO_7S_2$ |
| Chemical formula weight | 362.38 | 391.9 | 441.62 |
| Cell setting, space group | Triclinic, $P\bar{1}$ | Orthorhombic, $Pnma$ | Orthorhombic, $Pnma$ |
| $a, b, c$ (Å) | 7.8971 (8), 8.1750 (8), 11.2358 (11) | 9.5424 (11), 21.705 (2), 5.8137 (7) | 9.7662 (14), 22.080 (3), 5.9870 (8) |
| $\alpha, \beta, \gamma$ (°) | 73.945 (2), 83.063 (2), 83.435 (2) | 90, 90, 90 | 90, 90, 90 |
| $V$ (Å$^3$) | 689.48 (12) | 1204.1 (2) | 1291.0 (3) |
| $Z$ | 2 | 4 | 4 |
| $D_x$ (Mg m$^{-3}$) | 1.746 | 2.162 | 2.272 |
| Radiation type | Mo $K\alpha$ | Mo $K\alpha$ | Mo $K\alpha$ |
| $\theta$ range (°) | – | – | 3.53–29.97 |
| $\mu$ (mm$^{-1}$) | 0.793 | 4.854 | 3.427 |
| Temperature (K) | 293 (2) | 293 (2) | 293 (2) |
| Crystal form, color | Plate, colorless | Needle, colorless | Needle, colorless |
| Crystal size (mm) | $0.36 \times 0.20 \times 0.06$ | $0.23 \times 0.08 \times 0.06$ | $0.40 \times 0.07 \times 0.04$ |
| **Data collection** | | | |
| Diffractometer | Bruker Smart 1000 CCD area detector | Bruker Smart 1000 CCD area detector | Bruker Smart 1000 CCD area detector |
| Data collection method | Phi and omega scans | Phi and omega scans | Phi and omega scans |

**Table 1 (continued)**

| | (5) | (6) | (7) |
|---|---|---|---|
| No. of measured, independent and observed parameters | 3839, 2751, 2456 | 8022, 1792, 1529 | 6956, 1873, 1636 |
| Criterion for observed reflections | $I > 2\sigma(I)$ | $I > 2\sigma(I)$ | $I > 2\sigma(I)$ |
| $R_{int}$ | 0.0313 | 0.0254 | 0.0227 |
| $\theta_{max}$ (°) | 26.37 | 29.99 | 29.97 |
| Range of $h, k, l$ | $-9 \to h \to 9$ | $-13 \to h \to 12$ | $-10 \to h \to 13$ |
| | $-9 \to k \to 10$ | $-26 \to k \to 30$ | $-25 \to k \to 30$ |
| | $-14 \to l \to 13$ | $-8 \to l \to 7$ | $-8 \to l \to 7$ |
| | | | |
| Refinement | | | |
| Refinement on | $F^2$ | $F^2$ | $F^2$ |
| $R[F^2 > 2\sigma(F^2)]$, $wR(F^2)$, $S$ | 0.0343, 0.1011, 1.086 | 0.0225, 0.059, 1.029 | 0.0226, 0.0556, 1.013 |
| No. of reflections and parameters used in refinement | 2751, 194 | 1792, 98 | 1873, 98 |
| H-atom treatment | Mixed | Mixed | Mixed |
| Weighting scheme | $w = 1/[\sigma^2(F_o^2) + (0.0707P)^2 + 0.0000P]$, where $P = (F_o^2 + 2F_c^2)/3$ | $w = 1/[\sigma^2(F_o^2) + (0.0361P)^2 + 0.0000P]$, where $P = (F_o^2 + 2F_c^2)/3$ | $w = 1/[\sigma^2(F_o^2) + (0.0338P)^2 + 0.4684P]$, where $P = (F_o^2 + 2F_c^2)/3$ |
| $(\Delta/\sigma)_{max}$ | 0.002 | 0.001 | 0.001 |
| $\Delta\rho_{max}$, $\Delta\rho_{min}$ (e Å$^{-3}$) | 0.737, $-0.527$ | 0.517, $-0.476$ | 1.259, $-0.694$ |
| Extinction method | None | None | None |

Computer programs used: Bruker *SMART*, Bruker *SHELXTL*, *SHELXS*97, *SHELXL*97 (Sheldrick, 1997).

TGA: removal of water molecules at 380–400 K, 10.46% (calc. 25.79%), removal of naphthalene at 849–861 K.

### 3.5. [Ca$_2$(1,5-nds)(H$_2$O)$_2$] (5)

Calcium chloride anhydrous (0.11 g, 1 mmol) and disodium 1,5-nds (0.33 g, 1 mmol) were dissolved in distilled water (20 ml). The resulting solution was allowed to stand in an open beaker at room temperature. After ∼10 d, plate-like colorless crystals of (5) were collected (yield 25%, based on CaCl$_2$; found: C 32.98, H 2.46, S 18.07; C$_{10}$H$_{10}$CaO$_8$S$_2$ requires C 33.14, H 2.78, S 17.69%). TGA: release of water molecule at 397–626 K, 9.36% (calc. 9.93%), removal of naphthalene at 885–904 K.

### 3.6. [Sr(1,5-nds)(H$_2$O)] (6)

Strontium nitrate (0.11 g, 0.5 mmol) and disodium 1,5-nds (0.17 g, 0.5 mmol) were dissolved in distilled water (20 ml). The resulting solution was set out at room temperature in an open beaker. After ∼10 d colorless columnar crystals of (6) were collected [yield 44%, based on Sr(NO$_3$)$_2$; found: C 29.94, H 2.125; C$_{10}$H$_{10}$O$_8$S$_2$Sr requires C 29.30, H 2.46%]. TGA: release of water molecule at 569–594 K, 3.59% (calc. 4.59%), removal of naphthalene at 886–897 K.

### 3.7. [Ba(1,5-nds)(H$_2$O)] (7)

Barium acetate (0.13 g, 0.5 mmol) was dissolved in distilled water (25 ml), to which was added dropwise with constant stirring a solution of 1,5-nds acid (0.18 g, 0.5 mmol) in distilled water (20 ml). The resulting solution was allowed to stand in an open beaker at room temperature. After 2 d plate-like colorless crystals of (7) were collected [yield 42%, based on Ba(CH$_3$CO$_2$)$_2$; found: C 26.77, H 2.152; C$_{10}$H$_{10}$BaO$_8$S$_2$

requires C 26.13, H 2.19%]. TGA: release of water molecule at 537–575 K, 3.51% (calc. 4.07%), removal of naphthalene at 884–917 K.

## 4. Results and discussion

### 4.1. IR spectroscopy and TGA

The IR spectra for (0–(7) are shown in Fig. 1. The well resolved frequencies of naphthalene rings spans the regions 500–930 and 1500–1970 cm$^{-1}$. All compounds show strong bands at frequencies higher than 3300 cm$^{-1}$, corresponding to the presence of water molecules in all the compounds studied. For (1), there are two distinct sharp peaks at 3535 and 3480 cm$^{-1}$, indicating the two different hydrogen-bonding modes of the water molecules. There is a strong band at 3449 cm$^{-1}$ observed for (2), while for (3) the two sharp peaks are at 3578 and 3450 cm$^{-1}$, separated by 128 cm$^{-1}$. As we will see in the following discussion, the different splitting patterns of the O—H stretching vibrational peaks for these three compounds are consistent with the three different coordination and hydrogen-bonding modes adopted by the water molecules in (1)–(3). For (4) there is a strong, broad band around 3402 cm$^{-1}$, corresponding to extensive hydrogen bonding between the coordinated water molecules and the SO$_3^-$ groups. For (5) there are two, less well resolved bands at 3369 and 3425 cm$^{-1}$, respectively. For (6) absorption bands are weaker than those in the other compounds, occuring at 3577 and 3520 cm$^{-1}$. Finally, for (7) absorption bands occur at 3566 and 3499 cm$^{-1}$. Frequencies characteristic of the fundamental and split $\nu_3$ S—O stretching modes are observed in the range 1000–1200 cm$^{-1}$ (Smith *et al.*, 1998; Ohki *et al.*, 1985).

The TGA results show that the first weight loss takes place at 333–373 K, corresponding to the release of water molecules

**Table 2**
Selected bond distances (Å) and angles (°) for (1)–(7).

$[Li_2(C_{10}H_6S_2O_6)(H_2O)_2]$ (1)

| | | | |
|---|---|---|---|
| S1—O1 | 1.4579 (10) | Li1—O1 | 1.919 (3) |
| S1—O2 | 1.4456 (11) | Li1—O2$^i$ | 1.924 (3) |
| S1—O3 | 1.4572 (10) | Li1—O3$^{ii}$ | 1.994 (3) |
| Li1—O$w$ | 1.902 (3) | | |
| O$w$—Li1—O1 | 110.87 (13) | O1—Li1—O2$^i$ | 109.80 (12) |
| O$w$—Li1—O2$^i$ | 106.76 (13) | O1—Li1—O3$^{ii}$ | 106.54 (12) |
| O$w$—Li1—O3$^{ii}$ | 114.27 (13) | O2$^i$—Li1—O3$^{ii}$ | 108.56 (12) |

$[Na_2(C_{10}H_6S_2O_6)(H_2O)_2]$ (2)

| | | | |
|---|---|---|---|
| S1—O2 | 1.4472 (11) | Na1—O$w$ | 2.3687 (15) |
| S1—O1 | 1.4584 (12) | Na1—O1 | 2.3567 (13) |
| S1—O3 | 1.4619 (12) | Na1—O2$^{iii}$ | 2.3230 (13) |
| Na1—O$w^{iv}$ | 2.3636 (14) | Na1—O3$^v$ | 2.3185 (12) |
| O1—Na1—O$w$ | 95.62 (5) | O2$^{iii}$—Na1—O$w^{iv}$ | 169.72 (6) |
| O2$^{iii}$—Na1—O$w$ | 88.62 (5) | O2$^{iii}$—Na1—O1 | 87.69 (5) |
| O3$^v$—Na1—O$w$ | 133.26 (5) | O3$^v$—Na1—O1 | 130.82 (5) |
| O3$^v$—Na1—O$w^{iv}$ | 90.82 (5) | O3$^v$—Na1—O2$^{iv}$ | 88.41 (5) |
| O1—Na1—O$w^{iv}$ | 85.06 (5) | | |

$[K_2(C_{10}H_6S_2O_6)(H_2O)_2]$ (3)

| | | | |
|---|---|---|---|
| S1—O1 | 1.4511 (15) | K1—O1$^{vi}$ | 2.8751 (15) |
| S1—O2 | 1.4509 (16) | K1—O3$^{vi}$ | 2.8346 (17) |
| S1—O3 | 1.4520 (14) | K1—O$w$ | 2.789 (2) |
| K1—O1$^{vii}$ | 2.6693 (15) | K1—O$w^{vii}$ | 3.042 (2) |
| K1—O2 | 2.7339 (16) | K1—O$w^{viii}$ | 3.191 (2) |
| K1—O3$^{ix}$ | 2.7536 (14) | | |
| O1$^{vii}$—K1—O2 | 106.26 (5) | O$w$—K1—O1$^{vi}$ | 128.94 (6) |
| O1$^{vii}$—K1—O3$^{ix}$ | 88.29 (5) | O$w$—K1—O$w^{vii}$ | 130.20 (9) |
| O2—K1—O3$^{ix}$ | 134.53 (5) | O1$^{vii}$—K1—O$w^{vii}$ | 90.87 (6) |
| O1$^{vii}$—K1—O$w$ | 70.34 (6) | O2—K1—O$w^{vii}$ | 56.57 (5) |
| O2—K1—O$w$ | 84.24 (6) | O3$^{ix}$—K1—O$w^{vii}$ | 80.98 (5) |
| O3$^{ix}$—K1—O$w$ | 140.55 (6) | O3$^{vi}$—K1—O$w^{vii}$ | 128.72 (6) |
| O1$^{vii}$—K1—O3$^{vi}$ | 140.13 (5) | O1$^{vi}$—K1—O$w^{vii}$ | 80.56 (5) |
| O2—K1—O3$^{vi}$ | 100.89 (5) | O1$^{vii}$—K1—O$w^{viii}$ | 81.05 (5) |
| O3$^{ix}$—K1—O3$^{vi}$ | 93.08 (4) | O2—K1—O$w^{viii}$ | 143.27 (6) |
| O1$^i$—K1—O1$^{iii}$ | 159.610 (18) | O3$^{ii}$—K1—O$w^{iv}$ | 80.57 (5) |
| O2—K1—O1$^{vi}$ | 84.49 (5) | O3$^{vii}$—K1—O$w^{viii}$ | 60.01 (5) |
| O3$^{ix}$—K1—O1$^{vi}$ | 72.17 (5) | O1$^{vi}$—K1—O$w^{viii}$ | 100.87 (5) |
| O3$^{vi}$—K1—O1$^{vi}$ | 49.75 (4) | O$w$—K1—O$w^{viii}$ | 64.00 (7) |
| O$w$—K1—O3$^{vi}$ | 84.19 (6) | O$w^{vii}$—K1—O$w^{viii}$ | 160.03 (3) |

$[Mg(H_2O)_6](C_{10}H_6S_2O_6)$ (4)

| | | | |
|---|---|---|---|
| Mg—O1 | 2.0366 (8) | S—O4 | 1.4624 (9) |
| Mg—O2 | 2.1031 (7) | S—O5 | 1.4667 (8) |
| Mg—O3 | 2.0604 (8) | S—O6 | 1.4517 (8) |
| O1—Mg—O3$^x$ | 91.63 (3) | O3—Mg—O2$^x$ | 90.14 (3) |
| O1—Mg—O3 | 88.37 (4) | O6—S—O4 | 113.06 (5) |
| O1—Mg—O2 | 88.18 (3) | O6—S—O5 | 111.60 (5) |
| O3—Mg—O2 | 89.86 (3) | O4—S—O5 | 111.52 (5) |
| O1—Mg—O2$^x$ | 91.82 (3) | | |

$[Ca(C_{10}H_6S_2O_6)(H_2O)_2]$ (5)

| | | | |
|---|---|---|---|
| Ca—O2 | 2.3043 (12) | S1—O1 | 1.4558 (12) |
| Ca—O3 | 2.3107 (12) | S1—O2 | 1.4519 (12) |
| Ca—O5 | 2.3754 (12) | S1—O3$^{xi}$ | 1.4534 (13) |
| Ca—O6 | 2.3076 (12) | S2—O4 | 1.4392 (13) |
| Ca—O$w$1 | 2.3327 (13) | S2—O5 | 1.4686 (13) |
| Ca—O$w$2 | 2.3182 (13) | S2—O6$^{xii}$ | 1.4541 (12) |
| O2—Ca—O3 | 93.38 (5) | O6—Ca—O$w$1 | 83.44 (5) |
| O2—Ca—O6 | 177.50 (5) | O2—Ca—O$w$2 | 89.25 (5) |
| O6—Ca—O3 | 88.97 (5) | O3—Ca—O$w$2 | 94.22 (5) |
| O2—Ca—O5 | 83.70 (5) | O6—Ca—O$w$2 | 91.43 (5) |
| O3—Ca—O5 | 173.07 (5) | O$w$1—Ca—O5 | 86.00 (5) |
| O6—Ca—O5 | 93.87 (5) | O$w$2—Ca—O5 | 92.03 (5) |
| O2—Ca—O$w$1 | 95.78 (5) | O$w$2—Ca—O$w$1 | 174.36 (5) |
| O3—Ca—O$w$1 | 88.05 (5) | | |

$[Sr(C_{10}H_6S_2O_6)(H_2O)_2]$ (6)

| | | | |
|---|---|---|---|
| S—O1 | 1.4412 (15) | Sr—O2$^{xii}$ | 2.5700 (14) |
| S—O2 | 1.4533 (15) | Sr—O3$^{xiv}$ | 2.5531 (14) |
| S—O3 | 1.4536 (15) | Sr—O$w$ | 2.692 (2) |
| Sr—O1 | 2.5190 (14) | Sr—O$w^{xv}$ | 3.014 (3) |

| | | | |
|---|---|---|---|
| O1$^{xvi}$—Sr—O1 | 69.51 (7) | O3$^{xvii}$—Sr—O2$^{xiii}$ | 87.80 (5) |
| O1—Sr—O2$^{xiii}$ | 113.91 (6) | O1—Sr—O$w$ | 142.94 (4) |
| O1$^{xvi}$—Sr—O2$^{xiii}$ | 70.86 (5) | O2$^{xiii}$—Sr—O$w$ | 76.84 (6) |
| O1$^{xvi}$—Sr—O3$^{xiv}$ | 137.67 (6) | O3$^{xiv}$—Sr—O$w$ | 75.05 (6) |
| O1—Sr—O3$^{xiv}$ | 85.86 (6) | O1—Sr—O$w^{xv}$ | 66.13 (6) |
| O2$^{xiii}$—Sr—O2$^{xviii}$ | 80.02 (7) | O2$^{xiii}$—Sr—O$w^{xv}$ | 133.51 (4) |
| O3$^{xiv}$—Sr—O3$^{xvii}$ | 90.74 (7) | O3$^{xiv}$—Sr—O$w^{xv}$ | 72.60 (5) |
| O3$^{xiv}$—Sr—O2$^{xiii}$ | 151.25 (6) | | |

$[Ba(C_{10}H_6S_2O_6)(H_2O)_2]$ (7)

| | | | |
|---|---|---|---|
| S1—O1 | 1.447 (2) | Ba1—O2$^{xix}$ | 2.6698 (19) |
| S1—O2 | 1.437 (2) | Ba1—O3$^{xx}$ | 2.7229 (19) |
| S1—O3 | 1.446 (2) | Ba1—O$w$ | 2.880 (3) |
| Ba1—O1 | 2.6915 (19) | Ba1—O$w^{xxi}$ | 3.084 (3) |
| O1—Ba1—O1$^{xxii}$ | 91.82 (9) | O3$^{xx}$—Ba1—O3$^{xxiii}$ | 79.48 (9) |
| O1—Ba1—O3$^{xx}$ | 153.07 (8) | O1—Ba1—O$w$ | 74.98 (7) |
| O1$^{xxii}$—Ba1—O3$^{xx}$ | 88.46 (7) | O1—Ba1—O$w^{xxi}$ | 73.87 (9) |
| O2$^{xix}$—Ba1—O1 | 138.42 (9) | O3$^{xx}$—Ba1—O$w$ | 142.42 (5) |
| O2$^{xix}$—Ba1—O1 | 85.41 (8) | O2$^{xix}$—Ba1—O$w^{xxi}$ | 65.50 (8) |
| O2$^{xix}$—Ba1—O2$^{xxiv}$ | 70.40 (8) | O3$^{xx}$—Ba1—O$w$ | 79.11 (7) |
| O2$^{xix}$—Ba1—O3$^{xx}$ | 68.46 (7) | O3$^{xx}$—Ba1—O$w^{xxi}$ | 131.56 (6) |
| O2$^{xxiv}$—Ba1—O3$^{xx}$ | 111.70 (8) | O$w$—Ba1—O$w^{xxi}$ | 134.60 (6) |

Symmetry codes: (i) $x, -y + \frac{3}{2}, z + \frac{1}{2}$; (ii) $-x + 2, y - \frac{1}{2}, -z + \frac{3}{2}$; (iii) $x, -y + \frac{1}{2}, z - \frac{1}{2}$; (iv) $-x + 1, y - \frac{1}{2}, -z + \frac{3}{2}$; (v) $x, -y - \frac{1}{2}, z - \frac{1}{2}$; (vi) $-x, -y + 1, -z$; (vii) $x, -y + \frac{1}{2}, z + \frac{1}{2}$; (viii) $-x, -y, -z$; (ix) $-x, y - \frac{1}{2}, -z + \frac{1}{2}$; (x) $-x + 1, -y + 1, -z + 2$; (xi) $-x + 1, -y + 2, -z + 2$; (xii) $-x, -y + 1, -z + 2$; (xiii) $x - \frac{1}{2}, -y + \frac{1}{2}, -z + \frac{3}{2}$; (xiv) $x, y, z + 1$; (xv) $x + \frac{1}{2}, y, -z + \frac{5}{2}$; (xvi) $x, -y + \frac{1}{2}, z$; (xvii) $x, -y + \frac{1}{2}, z + 1$; (xviii) $x - \frac{1}{2}, y, -z + \frac{3}{2}$; (xix) $x, -y + \frac{3}{2}, z - 1$; (xx) $x - \frac{1}{2}, -y + \frac{3}{2}, -z + \frac{3}{2}$; (xxi) $x + \frac{1}{2}, y, -z + \frac{3}{2}$; (xxii) $x, -y + \frac{3}{2}, z$; (xxiii) $x - \frac{1}{2}, y, -z + \frac{3}{2}$; (xxiv) $x, y, z - 1$.

for (1)–(5). However, the process is incomplete for (1), (3) and (4) since the weight loss continues with increasing temperature and there are no obvious sharp phase changes. In the cases of (2) and (5) the temperature for removal of all water molecules is 655 and 626 K, respectively. The release of water from (6) and (7) occurs at much higher temperatures, 569 and 536 K, respectively. Finally, a large weight loss corresponding to the removal of organic groups was seen around 873 K in all the compounds.

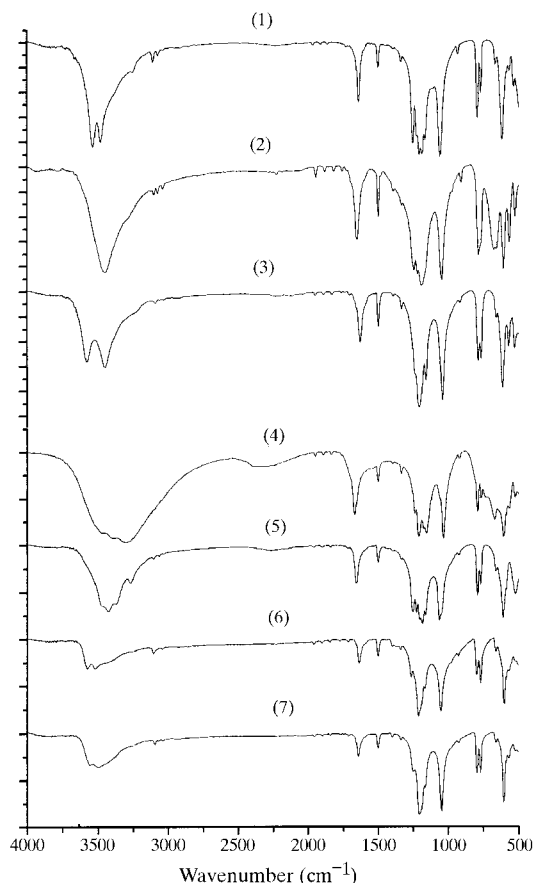### 4.2. Crystal structures of $[M_2(1,5\text{-nds})(H_2O)_2]$ ($M$ = Li$^+$, Na$^+$, K$^+$)

These three compounds crystallize in the same space group ($P2_1/c$), but are not isostructural. Despite the difference in the coordination behavior of the metal cations, their packing arrangements are very similar. The asymmetric unit consists of one metal cation, one water molecule and half a 1,5-naphthalenedisulfonate anion, which is related to the other half by an inversion center. All crystallize as a three-dimensional framework constructed by inorganic organic layers, with the metal–sulfonate inorganic portions pillared by the naphthalene rings.

**4.2.1. $[Li_2(1,5\text{-nds})(H_2O)_2]$ (1).** The coordination environment of Li$^+$ is shown in Fig. 2($a$). The Li atom is coordinated by one water molecule, Li—O$w$ 1.902 (3) Å, and three independent SO$_3^-$ groups with Li—O bond lengths of 1.919 (3), 1.924 (3) and 1.994 (3) Å. The two shorter Li—O1 and Li—O2 bonds involve two naphthalenedisulfonate groups in the same organic layer, while the longest bond (Li—O3) corresponds to that in an adjacent layer. The angular distribution around Li$^+$ is more uniform, ranging from 106.54 (12) to 114.27 (13)°. The coordination sphere of Li$^+$ can therefore be described as
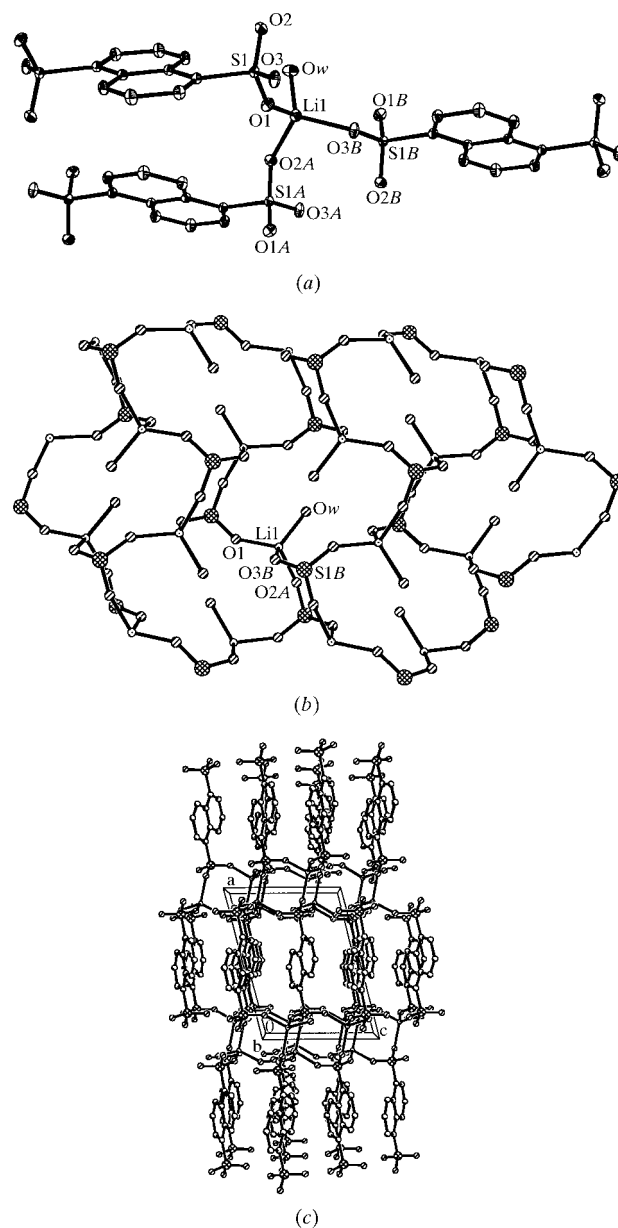
distorted tetrahedral. Each of the three $SO_3^-$ O atoms is coordinated to one $Li^+$ and the $SO_3^-$ group functions as a $\mu_3$-bridge, as shown in Fig. 2(b). The pleated inorganic sheet consists of two different rings sharing one edge. The first is a 16-membered ring constructed from four Li—O—S—O units, while the second is an eight-membered ring constructed from two L—O—S—O units. The $Li^+$ cations are situated above and below the (011) plane, with a foot-mean-square deviation of 0.89 Å. The pleating of the inorganic sheet leads the eight-membered rings to align along the $b$ axis, forming a channel running along that direction, as indicated in Fig. 2(c). Naphthalene rings align along the $b$ axis. The adjacent naphthalene rings aligning along the $c$ axis incline to each other at angles of 42.3°. The coordinated water molecules occupy the 16-membered rings, and form two strong hydrogen bonds with O atoms from two different $SO_3^-$ groups [$Ow\cdots O1$ 2.868 (2) Å, $\angle Ow—Hw\cdots O1$ 175 (2)°, $Ow—O3$ 2.894 (2) Å, $\angle Ow—Hw\cdots O3$ 153 (2)°].

**4.2.2. $[Na_2(1,5\text{-nds})(H_2O)_2]$ (2).** As shown in Fig. 3(a), the Na atom is five-coordinated by three different $SO_3^-$ groups and two water molecules in a distorted trigonal–bipyramidal fashion, with Na—O (water) distances of 2.364 (1) and 2.369 (2) Å. The distances to $SO_3^-$ are in the range 2.3185 (12)–2.3567 (13) Å, which are significantly longer than the lithium analog, and comparable with the reported Na—O

distances 2.293 (6)–2.555 (6) Å for $Na_2(H_2NC_{10}H_5$-$(SO_3)_2)_2\cdot5H_2O$ (Gunderman *et al.*, 1997). The equatorial angles range from 85.06 (5) to 133.26 (5)°, and the axial angle is 169.72 (6)°. As shown in Fig. 3(a), all the naphthalene rings lie to one side of the sodium center and belong to the same organic layer, while the water molecules are located on the other side and bridge to other sodium ions. Therefore, the inorganic portion is constructed by two layers of $Na^+$ ions located on planes parallel to the [011] direction, and the two sodium layers are held together by bridging water molecules. Sodiums in different layers of the same inorganic portion are
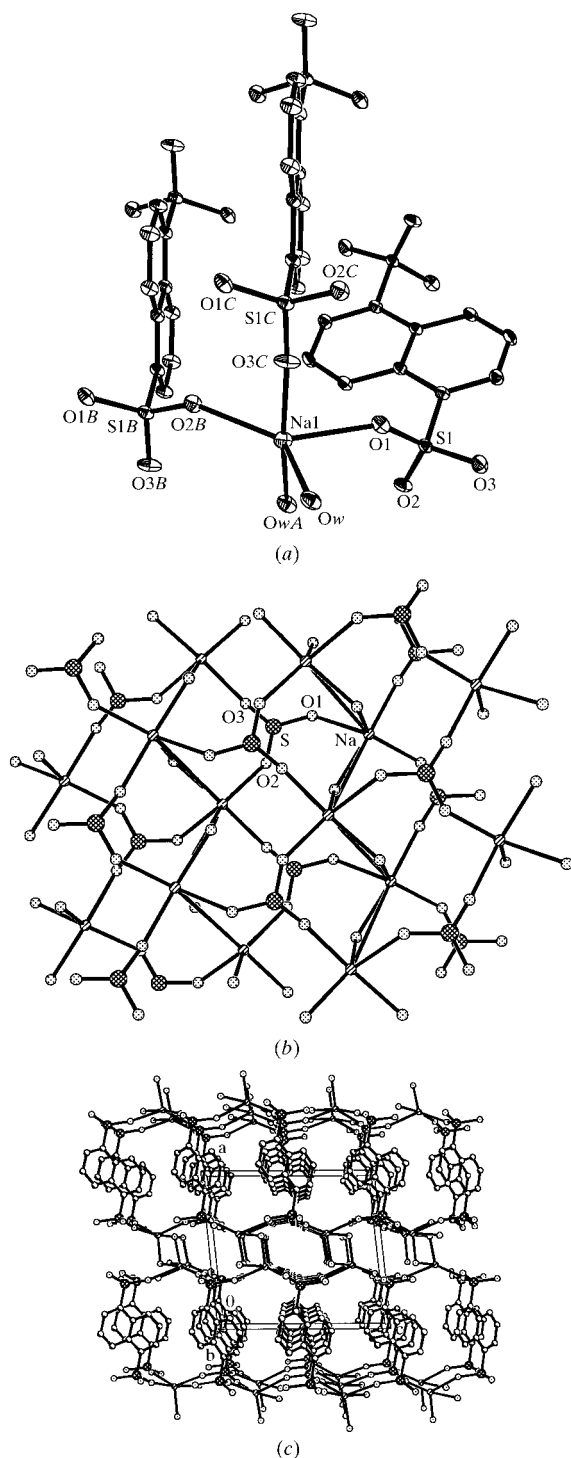


(a)



(b)



(c)

**Figure 2**
(a) Coordination environment of $Li^+$ in (1) with 30% probability displacement ellipsoids. The *A* and *B* sets of atoms are related to the primary one by the symmetry operations $x, -y+\frac{3}{2}, z+\frac{1}{2}$; and $-x+2, y-\frac{1}{2}, -z+\frac{3}{2}$, respectively; (b) The metal–sulfonate layered structure composed of two unique rings sharing one edge; (c) packing diagram along the $b$ axis.



**Figure 1**
IR spectra for (1)–(7).

coordinated by naphthalenedisulfonates which point in opposite directions along the $a$ axis, thus generating a three-dimensional structure. The projected inorganic sheet structure



(a)



(b)



(c)

**Figure 3**
(a) Coordination environment of Na$^+$ in (2) with 30% probability displacement ellipsoids. The $A$–$C$ sets of atoms are related to the primary one by the symmetry operations $-x + 1, y - \frac{1}{2}, -z + \frac{3}{2}$; $x, -y + \frac{1}{2}, z - \frac{1}{2}$; and $x, -y - \frac{1}{2}, z - \frac{1}{2}$, respectively; (b) the metal–sulfonate layered structure. Note that the two SO$_3^-$ groups are oriented below and above the plane, linking to six different Na$^+$ centers. (c) Packing diagram along the $b$ axis.

is shown in Fig. 3(b). Each of the SO$_3^-$ O atoms is coordinated to one Na$^+$ and the SO$_3^-$ group functions as a $\mu_3$-bridge, connecting three sodium centers, as shown in Fig. 3(b). The pleating of the inorganic portion creates large channels running along the $b$ axis, as shown in Fig. 3(c). The cross-section area is approximately $10.3 \times 5.5$ Å, if the portion occupied by water molecules is neglected. The naphthalene rings pack along the $b$ axis, while those of the adjacent pillars, along the $c$ axis, form dihedral angles of 79.9°. The coordinated water molecule is further involved in two hydrogen bonds with two different SO$_3^-$ groups [Ow$\cdots$O3 2.893 (2) Å, $\angle$Ow−H1$\cdots$O2 168 (3)°, and Ow$\cdots$O1 2.862 (2) Å, $\angle$Ow−H2$\cdots$O1 159 (3)°].

**4.2.3. [K$_2$(1,5-nds)(H$_2$O)$_2$] (3).** The coordination environment of (3) is shown in Fig. 4(a). The potassium atom is eight-coordinated by three water molecules, with distances of 2.789 (2), 3.042 (2) and 3.191 (2) Å, and five SO$_3^-$ oxygen atoms from four different groups with distances ranging from 2.669 (2) to 2.875 (2) Å, comparable to the reported K−O (SO$_3^-$) 2.691 (9)–2.966 (8) Å in K(H$_2$NC$_{10}$H$_6$SO$_3$)·H$_2$O (Gunderman & Squattrito, 1995). It is noted that the SO$_3^-$ groups linked to the same K$^+$ ion belong to two adjacent organic layers, the same as in the lithium compound. The O−K−O angles are distributed over a broad range, 49.75 (4)–159.61 (2)°. Two of the SO$_3^-$ oxygen atoms (O1 and O3) are each coordinated to two potassium ions, which makes the SO$_3^-$ group function as a $\mu_4$-bridge. The potassium ion is also coordinated by two O atoms belonging to an SO$_3^-$ group. The angle of the chelation ring O1−K−O3 is 49.75 (4)°. In other words, SO$_3^-$ functions both as a chelating and a bridging ligand in this compound, providing a total of five binding sites. This situation is different from (1) and (2). The water molecule is coordinated to three different K ions. The $\mu_4$-bridging and bidentate feature of the SO$_3^-$ group and the $\mu_3$-bridging feature of the water molecule construct a unique cage, as shown in the projected inorganic layer in Fig. 4(b). Fig. 4(c) shows the unique construction of the cage structure. All the K$^+$ cations are situated on a plane with a least-squares mean deviation of 0.26 Å. The naphthalenedisulfonates linked to K$^+$ are positioned above and below the K$^+$ plane and constitute a three-dimensional framework, as shown in Fig. 4(d). The arrangement of the inorganic portion is similar to that of the lithium compound, as shown in Fig. 2(c), except for the bridging feature of the water molecules. Naphthalene rings pack along the $b$ axis, while the rings of the adjacent pillars, along the $c$ axis, form a dihedral angle of 32.4°. The water molecule is involved in two hydrogen bonds with two SO$_3^-$ groups [Ow$\cdots$O2 2.751 (3) Å and $\angle$Ow−H1w$\cdots$O2 154 (3)°, and Ow$\cdots$O3 3.029 (3) Å, $\angle$Ow−H1wb$\cdots$O3 144 (3)°].

Although these three structures all contain one water molecule per metal atom, they show different coordination features: in (1) the water is coordinated to one lithium; in (2) it functions as a $\mu_2$-bridge; in (3) it is a $\mu_3$-ligand bridging three potassium centers. Furthermore, the coordination behavior of the SO$_3^-$ group is clearly different in (1)–(3). In (1) and (2), the SO$_3^-$ group provides three binding sites, while in (3) it provides five. The corresponding characteristic frequencies of O−H

stretching and S—O vibration in IR spectra demonstrate their differences in coordination behavior. The increase in coordination strength with decreasing charge/radius ratio is well illustrated in these three structures of Group 1 metals with large organic anions.

It is interesting to note that despite the difference in their coordination behavior and the changes in the metal–sulfonate inorganic portion of the structures, these three compounds adopt the same packing arrangement. All the naphthalene rings align along their $a$ axes, while the rings of adjacent pillars are inclined to each other. The layer structures are formed parallel to the $bc$ plane and extend along the $a$ axis. The interpillar distance (defined as the distance between the S atoms of adjacent pillars on the same edge) are half of the $c$ length (Figs. 2$c$, 3$c$ and 4$d$) and equal 4.03, 5.35 and 3.98 Å for (1), (2) and (3), respectively. The dihedral angles between the adjacent naphthalene rings are 42.3, 79.9 and 32.4°, respectively. Therefore, there is a correlation between the pillar distance and the dihedral angle; namely, the greater the separation the more inclined the naphthalene rings. This can be explained as

the result of rotation about the C—S single bond between the phenyl ring and the $SO_3$ group to bring the adjacent naphthalene rings into positions suitable for edge-to-face interactions. The thickness of the sum of inorganic and organic layers corresponds to the $a$ cell length, which is 10.89, 11.64 and 11.03 Å for (1), (2) and (3), respectively. Considering that the organic group is rather rigid, the difference is attributed largely to variations in the thickness of the inorganic layer. As mentioned above, for (2), the sodium ions are arranged as two separated layers bridged by water molecules in the inorganic portion, which makes the $Na^+$ compound the one with the thickest inorganic layer.

### 4.3. Crystal structures of $[M(1,5\text{-nds})(H_2O)_n]$ ($M$ = $Mg^{2+}$, $Ca^{2+}$, $Sr^{2+}$, $Ba^{2+}$)

**4.3.1. $[Mg(H_2O)_6](1,5\text{-nds})$ (4).** There is no direct coordination of $Mg^{2+}$ by the sulfonate O atoms. The cation is coordinated by six water molecules in a highly regular octahedron, with the Mg—O distances ranging from 2.0366 (8) to
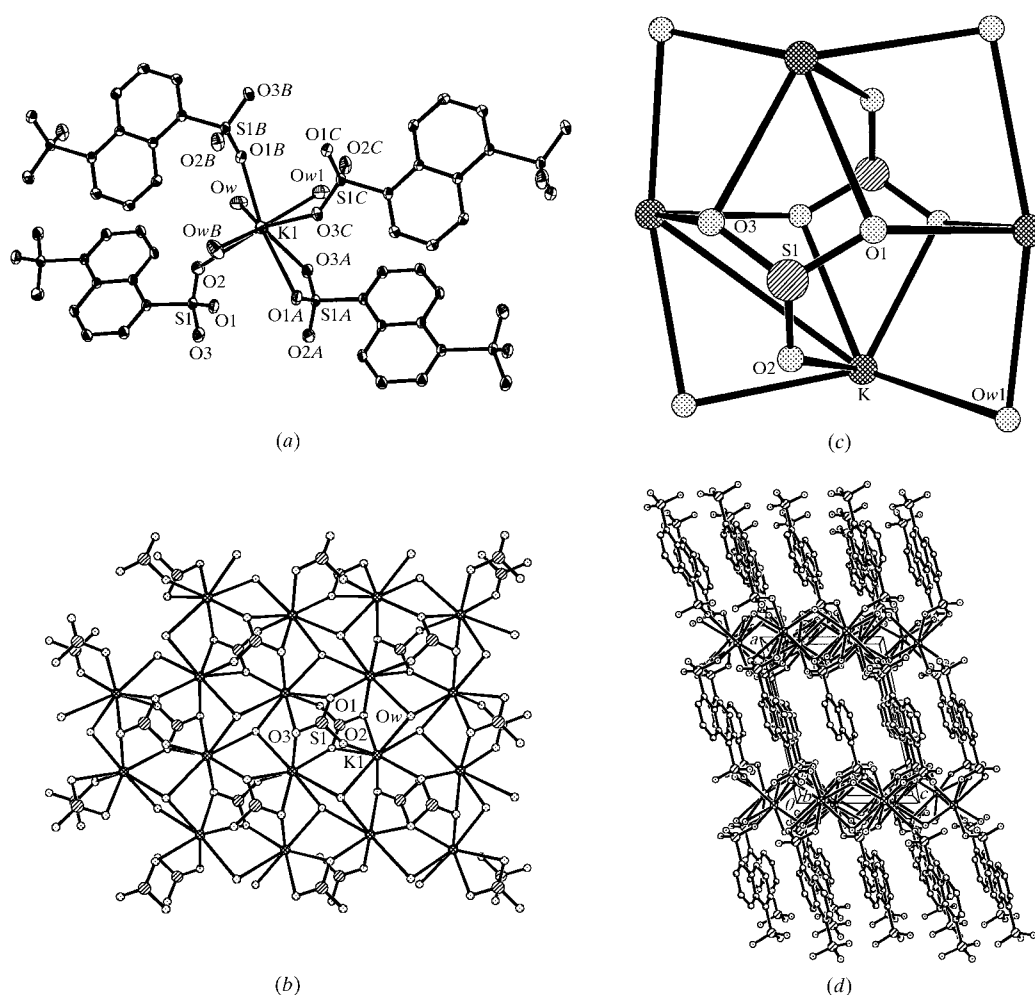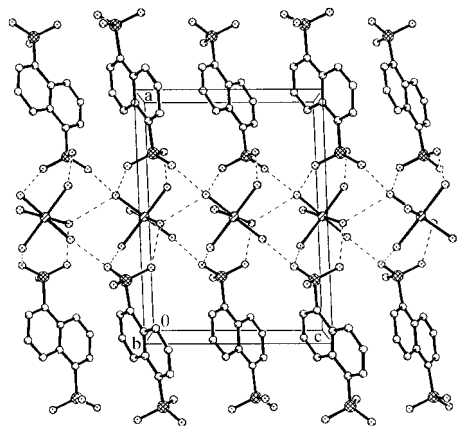


**Figure 4**
(a) Coordination environment of $K^+$ in (3) with 30% probability displacement ellipsoids. The sets of atoms $A$–$C$ are related to the primary one by the symmetry operations $-x$, $-y + 1$, $-z$; $x$, $-y + \frac{1}{2}$, $z + \frac{1}{2}$; and $-x$, $y - \frac{1}{2}$, $-z + \frac{1}{2}$, respectively. (b) The metal–sulfonate layered structure. Note the two $SO_3^-$ groups orienting below and above the plane, linking to four different $K^+$ centers. (c) The unique cage structure constructed by two $\mu_4$-$SO_3^-$ groups, four $K^+$ and four water molecules. (d) Packing diagram along the $b$ axis.

2.1031 (7) Å. The compound adopts a structure in which layers of organic anions alternate with layers of inorganic cations, as shown in Fig. 5. Each anionic layer contains naphthalene rings arranged so that the two $SO_3^-$ groups are directed to opposite edges of the layer. Between the anionic layers lie the hexaaquamagnesium cations. The naphthalene rings align along the *b* axis, while the adjacent rings along the *c* axis incline at 68.8°. A strong network of hydrogen bonds between the coordinated water molecules and the sulfonate O atoms hold the layers together. In addition, there are also hydrogen bonds between the coordinated water molecules in the same inorganic layer.

**4.3.2. [Ca(1,5-nds)(H₂O)₂] (5).** As shown in Fig. 6(*a*) the Ca ion is octahedrally coordinated by four $SO_3^-$ groups which form the basal plane, with Ca—O distances in the range 2.3043 (12)–2.3754 (12) Å, and two water molecules in the axial positions at distances of 2.3182 (13) and 2.3327 (13) Å, respectively. The *cis* bond angles range from 83.44 (5) to 95.78 (5)° and the *trans* bond angles range from 173.07 (5) to 177.50 (5)°. Each $SO_3^-$ group behaves as a $\mu_2$-ligand bridging two calcium centers, thus constructing a two-dimensional network with alternating organic–inorganic components, as shown in Fig. 6(*b*). The inorganic portion consists of two eight-membered rings with different conformations, represented as (Ca—O—S—O)₂, with Ca—Ca distances of 5.19 and 5.53 Å. All the $Ca^{2+}$ cations locate on a plane parallel to *ac*. Adjacent naphthalene rings in the same layer form a dihedral angle of 35.6° and the distance between the S atoms of adjacent pillars on the same edge is 5.5 Å. Layers are held closely together by four strong inter-layer hydrogen-bonding interactions formed between the coordinated water molecules and the free and coordinated $SO_3^-$ oxygen atoms (Fig. 6*c*), with $Ow\cdots O$ distances of 2.783 (2)–2.870 (2) Å and $Ow—Hw\cdots O$ angles of 164.9–177.2°.

There are two previously reported structures involving naphthalenesulfonate and calcium cations (Corbridge *et al.*, 1966; Brown *et al.*, 1984). In both cases, the $Ca^{2+}$ is hexahydrated and there is no direct interaction between $Ca^{2+}$ and the $SO_3^-$ group.

**4.3.3. [Sr(1,5-nds)(H₂O)] (6) and [Ba(1,5-nds)(H₂O)] (7).** Compound (6) adopts a three-dimensional framework as seen for (1)–(3). As shown in Fig. 7(*a*), the strontium ion is eight-coordinated by six different $SO_3^-$ groups, with Sr—O distances ranging from 2.5190 (14) to 2.5531 (14) Å, and two water molecules with Sr—O distances of 2.692 (2) and 3.014 (3) Å. The O—Sr—O angles are distributed over a broad range from 66.13 (6) to 151.25 (6)°. The six naphthalenedisulfonates coordinated to the same $Sr^{2+}$ center belong to two different organic layers. The inorganic layer structure is shown in Fig. 7(*b*). All the strontium ions are situated on the same least-squares plane, parallel to *ac*. Three strontium ions are bridged by two $\mu_3$-$SO_3^-$ groups below and above the strontium plane, giving rise to two 12-membered rings each represented as (Sr—O—S—O)₃. The binding of the $SO_3^-$ groups above and below the strontium plane generates small channels running along the *c* axis, which are filled by bridging water molecules, as indicated in Fig. 7(*c*). In the organic layer the naphthalene rings align along the *c* axis. Adjacent naphthalene rings along

(*a*)

(*b*)

(*c*)
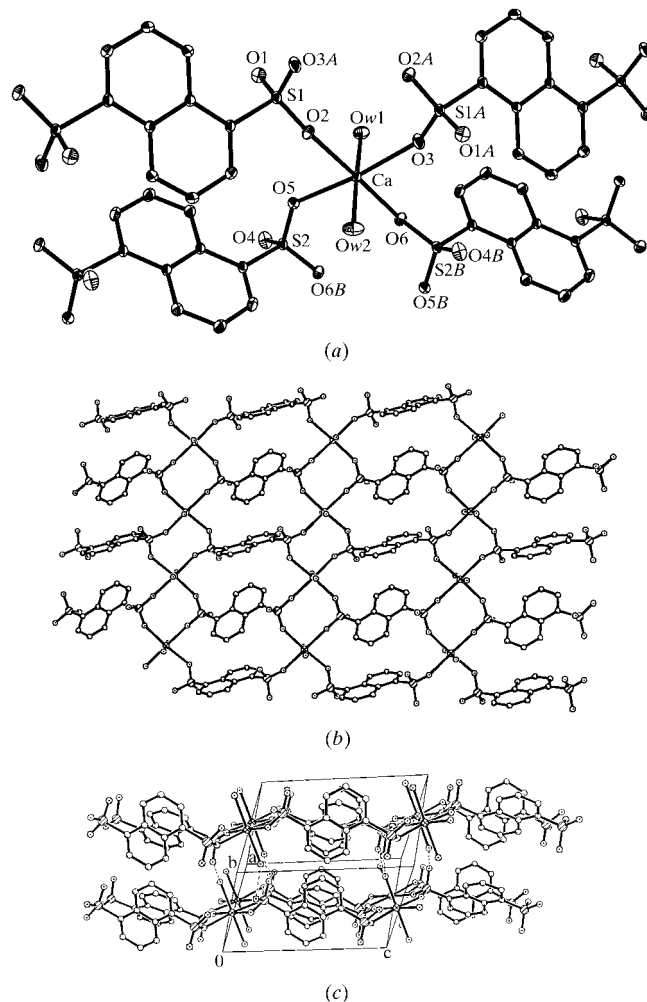
**Figure 6**
(*a*) Coordination environment of $Ca^{2+}$ in (5) with 30% probability displacement ellipsoids. The *A* set of atoms are related to the primary one by the symmetry operation $1 - x, -y, 2 - z$ and the *B* set by $-x + 1, -y, -z + 2$. (*b*) The two-dimensional inorganic–organic layered structure. (*c*) Packing diagram showing the inter-layered hydrogen bonds.

**Figure 5**
Unit-cell arrangement and hydrogen-bonding interactions observed in (4).

the *b* axis form a dihedral angle of 65.5° and the inter-pillar distance is 4.77 Å. There are two organic and two inorganic layers in the unit cell, which make the *b* axis much longer than that observed in the three-dimensional structures of (1)–(3). Furthermore, the propagating direction (*b* axis) of the layers is perpendicular to the plane defined by the strontium ions, giving rise to an orthorhombic system. The only obvious hydrogen bond observed in this structure is formed between the water molecule and one $SO_3^-$ oxygen [$Ow\cdots O1$ 3.047 (3) Å, with an unfavorable $Ow-Hw\cdots O1$ bond angle of 118 (3)°].

Compound (7) is isostructural with (6), with slightly longer cell axes. The $Ba-O(SO_3)$ distances range from 2.670 (2) to 2.723 (2) Å, while the $Ba-O(H_2O)$ distances lie between 2.880 (3) and 3.084 (3) Å. The $O-Ba-O$ angles range from 65.50 (8) to 153.07 (8)°.

Under the same reaction condition $Mg^{2+}$ forms a hexa-aquamagnesium cation instead of coordinating to the $SO_3^-$ group, while for the calcium compound two of the $SO_3^-$ oxygen atoms are coordinated to the $Ca^{2+}$ ion, and a two-dimensional network is constructed which is extended into a three-dimensional structure by strong inter-layer hydrogen bonding interactions. Note, however, that in the case of the $Sr^{2+}$ and $Ba^{2+}$ compounds, a three-dimensional structure similar to that observed for the 1 group is formed. Therefore, our above conclusion regarding the coordination strength of alkali and alkaline earth metal cations toward sulfonate, namely that alkali metal cations show a higher tendency to bond to $SO_3^-$ than alkaline earth cations, is consistent with our current observations. Finally, the increased coordination strength of Group 2 metal cations toward large organic anions as the charge/radius ratio decreases is clearly demonstrated by the structures of (4)–(7).

## 5. Conclusions

It was pointed out that the $Li^+$ ion is exceptionally small and therefore has an exceptionally high charge–radius ratio, comparable to that of $Mg^{2+}$. The properties of a number of lithium compounds are therefore anomalous in relation to other Group 1 elements, while resembling those of magnesium compounds (Cotton & Wilkinson, 1988). However, in these Group 1 and Group 2 1,5-naphthalenedisulfonate compounds, $Li^+$ is coordinated by three different $SO_3^-$ groups and forms a stable three-dimensional network analogous to that of $Na^+$ and $K^+$, while $Mg^{2+}$ does not interact with the $SO_3^-$ group. However, as the charge/radius ratio decreases, the coordination strength of Group 1 metal ions toward arenedisulfonate increases in the order $Li^+ < Na^+ < K^+$. This trend is seen in the coordination numbers of 4, 5 and 8 for $Li^+$, $Na^+$ and $K^+$, respectively, in the solid-state structures of [$M_2$(1,5-nds)(H_2O)_2$] even though these crystallize in the same space group, have the same stoichiometry and exhibit similar packing arrangements. In contrast, it is surprising that under the same reaction condition, $Mg^{2+}$ is not coordinated by the $SO_3^-$ group, as reported for two other $Mg^{2+}$ naphthalene-sulfonate salts (Wang *et al.*, 1994; Cody & Hazel, 1977).

The three-dimensional structures adopted by (1)–(3) and (6)–(7) are reminiscent of the reported copper and zinc bis(phosphonates) (Poojary *et al.*, 1996, 1997, and references cited therein), as well as to the [$G_2$(1,5-nds)(G)] host structure (Russell *et al.*, 1997), in which the guanidinium ion (G) takes the place of a metal ion and the three-dimensional pillared framework is constructed by ionic hydrogen bonds formed between the $SO_3^-$ O atoms and amino H atoms of the guanidinium cation. As a result of direct coordination between the metal center and the $SO_3^-$ oxygen atoms, the cavities created by the metal system are much smaller than that of the guanidinium system, in which the adjacent pillars are separated by two $N-H$ which are hydrogen-bonded to the same $SO_3^-$ O atom. Furthermore, the adjacent naphthalene rings in the [$G_2$(1,5-nds)(G)] host structure are oriented face-to-face parallel to each other and create enough space for guest molecules. Nevertheless, the metal systems have much higher thermal stability as the result of the covalent nature of the solid-state structures.



*(a)*



*(b)*



*(c)*
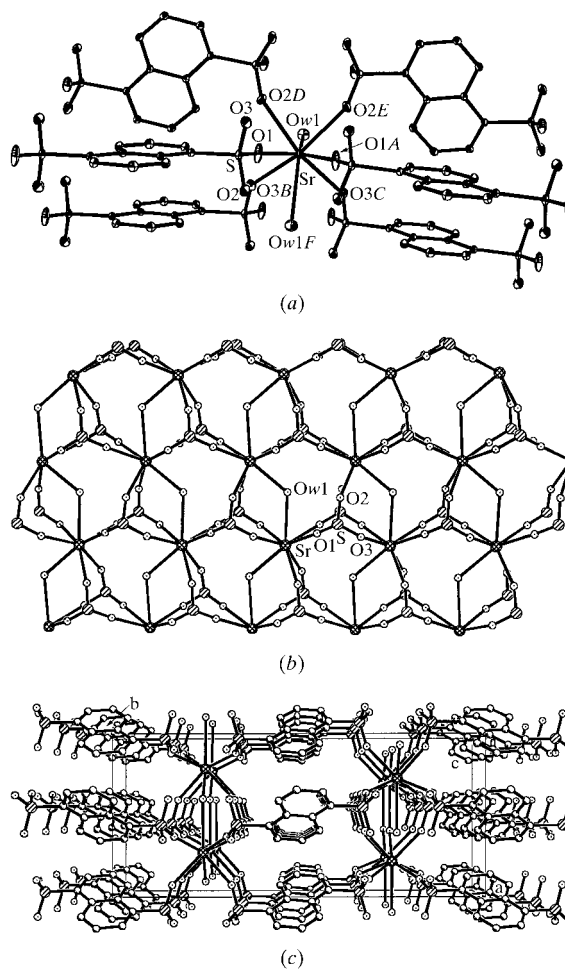
**Figure 7**
(*a*) Coordination environment of $Sr^{2+}$ in (6) with 30% probability displacement ellipsoids. The *A*–*F* sets of atoms are related to the primary ones by the operations $A: x, -y+\frac{1}{2}, z$; $B: x, y, z+1$; $C: x, -y+\frac{1}{2}, z+1$; $D: x-\frac{1}{2}, -y+\frac{1}{2}, -z+\frac{3}{2}$; $E: x-\frac{1}{2}, y, -z+\frac{3}{2}$; $F: x+\frac{1}{2}, y, -z+\frac{5}{2}$, respectively. (*b*) The two-dimensional metal–sulfonate layered structure. Note that the two $SO_3^-$ groups lie below and above the plane, linking three $Sr^{2+}$ centers. (*c*) Packing diagram along the *b* axis.

# research papers

The organic pillars in these structures are closely packed. However, it is noted that all the three-dimensional compounds contain metal-coordinated water molecules which are easily removed upon heating. This treatment will leave vacant metal coordination sites which maybe accessible to other species for intercalation or serve as reaction sites, a phenomenon which has been reported for metal phosphates (Poojary & Clearfield, 1995; Cao *et al.*, 1993). Furthermore, by introducing smaller spacer groups between the disulfonate pillars in the cross-linked structures, it is possible to create pores in these compounds (Dines *et al.*, 1983; Alberti *et al.*, 1993; Poojary *et al.*, 1994). Further experiments are being conducted along these lines in order to explore the potential applications of pillared metal sulfonates, as well as to compare the similarities, and differences, with the well documented phosphates.

## References

Alberti, G., Costantino, U., Marmottini, F., Vivani, R. & Zappelli, P. (1993). *Angew. Chem. Int. Ed. Engl.* **32**, 1357–1359.

Alcock, N. W., Kemp, T. J. & Leciejewicz, J. (1993). *Inorg. Chim. Acta*, **203**, 81–86.

Blessing, R. (1995). *Acta Cryst.* A**51**, 33–38.

Brown, C. J., Ehrenberg, M. & Yadav, H. R. (1984). *Acta Cryst.* C**40**, 58–60.

Bruker (1998*a*). *SMART*, Version 5.0. Bruker AXS, Madison, Wisconsin, USA.

Bruker (1998*b*). *SHELXTL*, Version 5.1. Bruker AXS, Madison, Wisconsin, USA.

Bruker (1999). *SAINT*, Version 6.0. Bruker AXS, Madison, Wisconsin, USA.

Cai, J., Chen, C.-H., Liao, C.-Z., Yao, Y.-H., Hu, X.-P. & Chen, X.-M. (2001). *J. Chem. Soc. Dalton Trans.* pp. 1137–1142.

Cao, G., Lynch, V. M. & Yacullo, L. N. (1993). *Chem. Mater.* **5**, 1000–1006.

Cody, V. & Hazel, J. (1977). *Acta Cryst.* B**33**, 3180–3184.

Corbridge, D. E. C., Brown, C. J. & Wallwork, C. (1966). *Acta Cryst.* **20**, 698–699.

Cotton, F. A. & Wilkinson, G. (1988). *Advanced Inorganic Chemistry*, 5th ed., pp. 124, 133. New York: Wiley Interscience.

Côté, A. P. & Shimizu, G. K. H. (2001). *Chem. Commun.* pp. 251–252.

Dines, M. B., Cooksey, R. E., Griffith, P. C. & Lane, R. H. (1983). *Inorg. Chem.* **22**, 1003–1004.

Gunderman, B. J., Kabell, I. D., Squattrito, P. J. & Dubey, S. N. (1997). *Inorg. Chim. Acta*, **258**, 237–246.

Gunderman, B. J. & Squattrito, P. J. (1994). *Inorg. Chem.* **33**, 2924–2931.

Gunderman, B. J. & Squattrito, P. J. (1995). *Inorg. Chem.* **34**, 2399–2406.

Kosnic, E. J., McClymont, E. L., Hodder, R. A. & Squattrito, P. J. (1992). *Inorg. Chim. Acta*, **201**, 143–151.

Ohki, Y., Suzuki, Y., Nakamura, M., Shimoi, M. & Ouchi, A. (1985). *Bull. Chem. Soc. Jpn*, pp. 2968–2974.

Poojary, D., Zhang, B., Bellinghausen, P. & Clearfield, A. (1996). *Inorg. Chem.* **35**, 4942–4949.

Poojary, D., Zhang, B. & Clearfield, A. (1994). *Angew. Chem. Int. Ed. Engl.* **33**, 2324–2326.

Poojary, D. M. & Clearfield, A. (1995). *J. Am. Chem. Soc.* **117**, 11278–11284.

Poojary, D. M., Zhang, B. & Clearfield, A. (1997). *J. Am. Chem. Soc.* **119**, 12550–12559.

Russell, V. A., Evans, C. C., Li, W. & Ward, M. D. (1997). *Science*, **276**, 575–579.

Sheldrick, G. M. (1997). *SHELX*97. University of Göttingen, Germany.

Shimizu, G. K. H., Enright, G. D., Ratcliffe, C. I., Rego, G. S., Reid, J. L. & Ripmeester, J. A. (1998). *Chem. Mater.* **10**, 3282–3283.

Shimizu, G. K. H., Enright, G. D., Ratcliffe, C. I., Preston, K. F., Reid, L. & Ripmeester, J. A. (1999). *Chem. Commun.* pp. 1485–1486.

Shimizu, G. K. H., Enright, G. D., Ratcliffe, C. I. & Ripmeester, J. A. (1999). *Chem. Commun.* pp. 461–462.

Shubnell, A. J., Kosnic, E. J. & Squattrito, P. J. (1994). *Inorg. Chim. Acta*, **216**, 101–102.

Smith, G., Cloutt, B. A., Lynth, D. E., Byriel, K. A. & Kennard, C. H. L. (1998). *Inorg. Chem.* **37**, 3236–3242.

Sundberg, M. R. & Sillanpää, R. (1993). *Acta Chem. Scand.* **47**, 1173–1178.

Thompson, M. E. (1994). *Chem. Mater.* **6**, 1168–1175.

Wang, J.-L., Li, B. & Miao, F.-M. (1994). *Jiegou Huaxue (J. Struct. Chem.)* **13**, 304–306.

Yu, J. O., Côté, A. P., Enright, G. D. & Shimizu, G. K. H. (2001). *Inorg. Chem.* **40**, 582–583.